 CMC, vol.23, no.2, pp.101-117, 2011

Molecular Design of the Solid Copolymer Electrolyte-Poly(styrene-b-ethylene oxide) for Lithium Ion Batteries

Cheng-Hung San[1] **and Che-Wun Hong**[1,2]

Abstract: Poly(ethylene oxide) (PEO) is a commonly used electrolytic polymer in lithium ion batteries because of its high viscosity which allows fabricating thin layers. However, its inherent low ionic conductivity must be enhanced by the addition of highly conductive salt additives. Also its weak mechanical strength needs a complementary block, such as poly(styrene) (PS), to strengthen the electrolytic membrane during charging/discharging processes. PS is a strong material to complement the PEO and to create a reinforced copolymer electrolyte termed as the poly(styrene-b-ethylene oxide) (PS-PEO). In this work, molecular dynamics simulations are employed to study the effects of doping the PS constituents into the PEO based copolymer electrolyte. The results reveal that strengthening the mechanical strength increases the intra conjugation forces which penalize the ionic conductivity. Hence both ionic conductivity and mechanical strength of the copolymer have to be compromised. This paper designs the optimized molecular structure through the atomistic analysis instead of try-and-error experiments.

Keywords: Lithium ion batteries, Polymer electrolyte, Molecular dynamics, PS-PEO

1 Introduction

In the green energy storage or power generation devices, electrolytic membranes are designed to provide the diffusion path of delegate ions and to prevent electron flow between the anode and the cathode. Poly(ethylene oxide) (PEO) was employed for lithium ion transportation in both crystalline and amorphous phases [Gadjourova, Andreev, Tunstall, and Bruce (2001); Andreev and Bruce (2000)]. Doping an aliovalent anion (SiF_6^{2-}) into the PEO and the addition of the PEO side

[1] Department of Power Mechanical Engineering , National Tsing Hua University, Hsinchu 30013, Taiwan

[2] Corresponding author: Phone: +886-3-5742591; Fax: +886-3-5722840; E-mail:cwhong@pme.nthu.edu.tw

chains were proposed to enhance the initial ionic conductivities [Brandell, Liivat, Kasema, Aabloo, and Thomas (2005); Liivat, Brandell, and Thomas (2007); Hektor, Klintenberg, Aabloo, and Thomas (2003)]. Apart from the molecular structure, thermodynamic properties of the PEO had been thoroughly investigated in previous works [Fullerton-Shirey and Maranas (2009); Ennari, Neelov, and Sundholm (2000); Ennari, Pietila, Virkkunen, and Sundholm (2002); Borodin, Douglas, Smith, Trouw, and Petrucci (2003)]. Neutron spin echo (NSE) technique was utilized to measure the collective dynamics in PEO samples experimentally [Brodeck, Alvarez, Arbe, Juranyi, Unruh, Holderer, Colmenero, and Richter (2009)].

Evaluation of the mechanical strength in the PEO sulfonic acid-based polymer was further investigated by an atomic level analysis [Grujicic, Chittajallua, Cao, and Roy (2005)]. Also, by varying the ethylene oxide (EO) ratio and adding highly conductive salt additives, a remarkable slowing down of polymer relaxation was discovered [Siqueira and Ribeiro (2005); Siqueira and Ribeiro (2005)]. Extensive research for understanding the ionic transport mechanism was conducted using both experimental spectroscopy and computational quantum chemistry [Karan, Pradhan, Thomas, Natesan, and Katiyar (2008); Diddens, Heuer, and Borodin (2010); Ogawa, Miyano, Suzuki, Suzuki, Tsuboi, Hatakeyama, Endou, Takaba, Kubo, and Miyamoto (2010)]. The molecular strength in the PEO electrolyte was evaluated by comparing a set of molecular simulations of the uni-axial deformation under constant stress-rate conditions. They showed that the PEO exhibited a low mechanical strength [Yang, Shi, Pramoda, Goh (2007)].

Copolymer designs are an effective measure to enhance the stiffness, strength, ductility, and toughness of the polymer electrolytes. In which, poly(styrene-b-ethylene oxide) (PS-PEO) received high attention recently. The weak mechanical strength of the PEO needs a complementary block, such as the poly(styrene) (PS). A synthetic method was proposed by Boschet et al. to fabricate PS-block-PEO associative water-soluble polymers [Boschet, Branger, and Margaillan (2003)]. Microphase-separated PS-PEO thin films were used to investigate the transition behavior between crystallization and micro-phase separation in the di-block thin film material [Yang and Han (2009); Neto, James, and Telford (2009); Yang, Yu, and Han (2010)]. Polymerization of the ethylene oxide initiated by lithium derivatives in the PS-PEO was also studied. Experimental approaches were employed to optimize the PS-PEO characteristics [Rejsek, Desbois, Deffieux, and Carlotti (2010); Young and Epps (2009)]. However, they are normally based on try-and-error and make the research work time-consuming and tedious.

Molecular dynamics (MD) analysis is a widely used method to directly observe the atomic transport in various applications [Li, Saheli, Khaleel, and Garmestani (2006); Lee and Hong (2009); Chen and Hong (2011)]. This paper intends to use

molecular dynamics simulations to investigate the lithium ion transport phenomena in the proposed PS-PEO copolymer electrolyte. The atomistic technique can be used to find the equilibrium PS/PEO mixture that meets the required ionic conductivity with satisfactory mechanical strength.

2 Simulation System and Molecular Models

2.1 Simulation System

A molecular simulation system with a unit cell volume of 25Å $\times$ 25Å $\times$ 25Å contains mainly the backbone of the PEO and the dopant PS in various percentages. To measure the PS additive effect in the polymer electrolyte, PS weight percents (wt%) from 0% to 70% were setup. Salts for improving the ionic conductivity are also included in the simulation system. A dissociation state containing the lithium ions (Li^+) and phosphorus fluorides (PF_6^-) chemical compounds which form the salt, $LiPF_6$, are input in the system, alongside 250 water molecules. The first step is to pre-optimize the molecular structure using a semi-empirical quantum based simulation method [Hypercube, 2002], which optimizes the structure geometry and evaluates the charge distribution. The optimized structure and charge equilibrium states are then exported to a molecular dynamics simulation platform (DL_POLY) [Smith, Leslie, and Forester (2003)] to predict the phase-space trajectories of active ions. The simulation volume equals to 1.5625×10^4 Å^3 while the system density for the PEO corresponds to 0.9755 g.cm^{-3}. For PS-PEO, the density has a range from 0.9693 to 1.0137 g.cm^{-3}, depending on the different PS wt%. The molar concentration of the salt additives corresponds to a typical experimental condition which normally conducted at the molar concentration equal to 1 M.

2.2 Molecular Models

In a Hamiltonian system, the total energy (E) is composed by three energy components, namely; the intra-molecular potential (U_{intra}), the inter-molecular potential (U_{inter}), and the kinetic energy (K). It is expressed by:

$$E = U_{intra} + U_{inter} + K \tag{1}$$

Regarding multi-atom systems, there are mainly three types of intra- molecular potentials.

$$U_{intra} = U_{angle} + U_{bond} + U_{dihedral} \tag{2}$$

where U_{angle} is called the valence angle potential, U_{bond} is the bond potential, and $U_{dihedral}$ is defined as the dihedral angle potential. Under microcanonical (NVE)

ensemble, the Hamiltonian (H) is a constant and the system dynamics is expressed by:

$$H_{NVE}(r,p) = E = K(r,p) + U(r) \tag{3}$$

where E is the total energy, r represents the instantaneous position, p represents the conjugate momenta, $K(r,p)$ denotes the kinetic energy, and $U(r)$ represents the potential energy. A canonical NVT (constant particle number, constant volume and constant temperature) simulation using the Nose thermostats from the NVE ensemble, based on the NVE Hamiltonian can be written as:

$$H_{NVT} = H_{NVE} + \frac{s^2 P_s^2}{2Q_{mass}} + \frac{N \ln s}{\beta} \tag{4}$$

where$s$ is the Helmholtz free energy of the system, P_s is the momentum thermostat degrees of freedom, Q_{mass} is the effective mass, N is the number of particles, β equals to $(k_B T)^{-1}$, and k_B is the Boltzmann constant To evaluate the mechanical strength inside the polymer structure, a constant strain approach is employed in this study. The approach starts from expanding the dimensions of the unit cell then re-scaling the new coordinates of the atoms in a new dimension. Generally, the stress in a solid polymer is estimated from the response function of its total energy. The stress tensor, σ_{ij}, can be derived as:

$$\sigma_{ij} = \frac{1}{V}\left(\frac{\partial E}{\partial \varepsilon_{ij}}\right) \tag{5}$$

where V is the volume of the solid, E is the total energy, and ε_{ij} is the strain tensor. In the atomistic scale, the equation of total energy is transformed to be:

$$E = K + U = \frac{1}{2} M v^2 + U(r) \tag{6}$$

where K is the kinetic energy, U is the potential energy, M is the mass of the atom, v is the magnitude of velocity, $U(r)$ is the potential energy at the atom location r. Therefore, the stress tensor can be calculated at each strain increment by:

$$\sigma_{ij} = -\frac{1}{V}\left(\sum M v_i v_j + \sum F_i r_j\right) \tag{7}$$

where F is the inter atomic force, and subscripts i, j denote the atom number. This stress tensor can also be calculated by an alternative continuum-molecular form

derived by Shen and Atluri (2004). The ionic conductivity (λ) according to the Einstein relation can be expressed by:

$$\lambda = \frac{e^2}{6tVK_BTN}\sum_{ij}^{N} z_i z_j < [R_i(t) - R_i(0)][R_j(t) - R_j(0)] > \tag{8}$$

where e denotes the electron charge, t represents elapsed time, V represents the volume, K_B is the Boltzmann constant, T is temperature, N the total atom number, z represents the charge, and$R$ denotes the displacement.

The Dreiding forcefield proposed by Mayo, Olfason, and Goddard (1990) with harmonic valence and cosine-Fourier expansion torsion is adopted in this work. In which, the van der Waals force is described by the typical 12-6 Lennard-Jones function, and the hydrogen bonding is expressed by an explicit 12-10 Lennard-Jones relation. Electrostatic properties are characterized by monopoles and a screened Coulombic force. The total potential consists of inter and intra potentials and the inter-molecular potential comprises of the van der Waals potential and the electrostatic potential. A rigid three-site SPC/E model [Berendsen, Grigera, and Straatama (1987)] is used for water molecules. A SHAKE algorithm [Ryckaert, Ciccotti, and Berendsen (1977)] is employed in order to keep the covalent bond rigid for molecules. An Eward summation [Allen and Tildesley (1987)] is adopted to calculate the electrostatic potential in the periodic boundary conditions. In the simulation process, an initial 10 ps time interval is used to reach the system energy equilibration. Then, an additional 40 ps period of NVT ensemble is conducted. The equations of motion are calculated by the Verlet scheme [Verlet (1967)] with 1 fs time step. The Lennard-Jones and electrostatic potential have a cut-off radius at 10 Å. The operational temperatures are controlled and maintained within a ± 5 percentage fluctuation during the simulation. Molecular dynamics simulations are carried out on the DL_POLY [Smith, Leslie, and Forester (2003)] platform to predict the ionic conductivity and to evaluate the mechanical strength in the polymer electrolyte. The simulation conditions and input data are summarized and displayed in Table 1.

3 Simulation Results and Discussion

Figure 1 (a) and Figure 1 (b) show the chemical compositions of the PEO and the PS-PEO, respectively. Their optimized molecular structures are evaluated and shown in Figure 2. Lithium phosphorus fluorides ($LiPF_6$) in Figure 3 are used as the salt additives. The molecular structure and the charge distribution of the salt additive are shown. The whole molecular system structure of the simulation system is shown in Figure 4. The study starts from the effect of the PS addition to the PEO based polymer electrolyte.

Table 1: Summary of simulation conditions and input data

	PEO	PS-PEO
Volume ($Å^3$)	$1.5625x10^4$	$1.5625x10^4$
Density (gcm^{-3})	0.9755	0.9693∼1.0137
$LiPF_6$ concentration (M)	1	1
Canonical ensemble	NVT	NVT
Simulation time step (fs)	1	1
Simulation time period (ps)	50	50

(a)

$[CH_2\text{-}CH_2\text{-}O]_n\text{-}CH_3$

(b)

$[CH_2\text{-}CH]_m\text{-}[CH_2\text{-}CH_2\text{-}O]_n\text{-}CH_3$

Figure 1: The chemical compositions of (a) poly(ethylene oxide) (PEO) and (b) poly (styrene- b-ethylene oxide) (PS-PEO); m, n are repetition numbers.

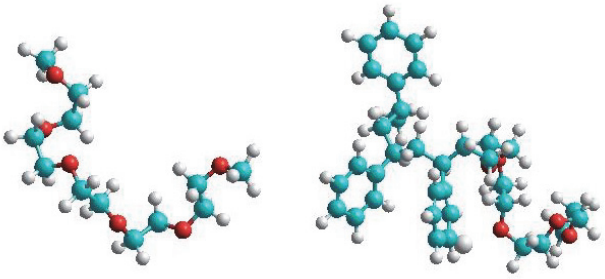

Figure 2: Optimized molecular structures of the PEO and the PS-PEO

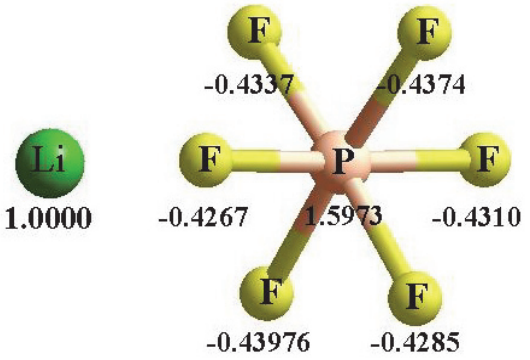

Figure 3: Molecular structure of the lithium phosphorus fluorides ($LiPF_6$) and the charge distribution

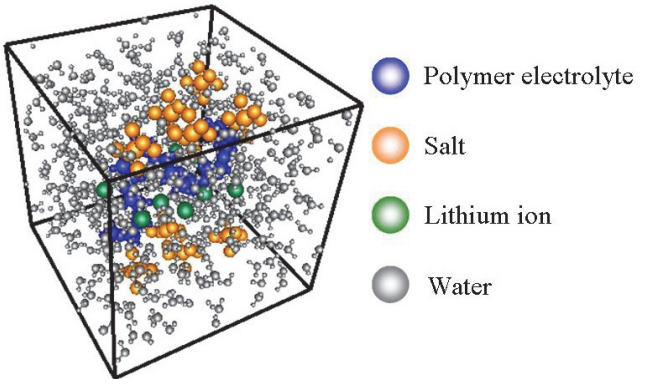

Figure 4: Simulation system of the polymer electrolyte with salts, lithium ions and water molecules

Figure 5 shows the total energy distributions of PEO and PS-PEO in the simulation period. It is noted that the PEO exhibits a higher energy level than that in the PS-PEO. The reason is because the PEO based material performs a swifter activation than the PS-PEO, which has a higher molecular weight due to the PS constituents. The thermal effect on the copolymer characteristics is significant with different PS wt%. Further calculations on the material characteristics under different temperatures and PS wt% are discussed in the later sections.

Figure 6 shows the mean square displacements (MSD) of lithium ions in the PEO and in the PS-PEO, where the atomic movements increase with the simulation period. Comparing the simulation result, it conspicuously shows that the movement

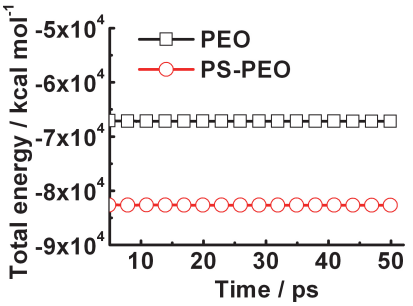

Figure 5: Total energy distributions of PEO and PS-PEO in the simulation period

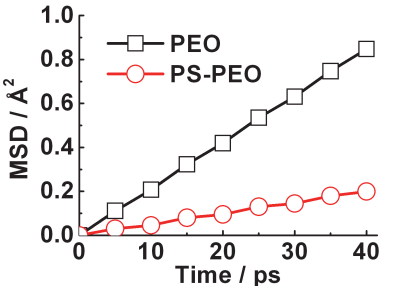

Figure 6: Mean square displacements (MSD) of lithium ions in the PEO and in the PS-PEO. The diagram indicates that the PEO exhibits a higher diffusion coefficient than the PS-PEO.

of lithium ion through PEO is higher than that in the PS-PEO. The diffusion coefficients of lithium ions, shown in Figure 7, vary with different temperature conditions. Indeed, the ionic transportation through PEO occurs at a higher rate than that in the PS-PEO because the ionic behavior in PEO oscillates more fiercely under the thermal effects. Figure 8 shows the Arrhenius plot of Li ions in the PEO and in the PS-PEO electrolyte, respectively. Another simulation result is obtained from Siqueira and Ribeiro (2006). The experimental result is extracted from Gorecki, Andreani, Berthier, Armand, Mali, Roos, and Brinkmann (1986). They show good agreement.

The PEO based polymer electrolyte shows an ionic conductivity of about 10^{-4} to 10^{-5} S.cm^{-1}, while the PS-PEO distributes on the range of 10^{-6} to 10^{-5} S.cm^{-1}. At room temperature conditions, the PEO exhibits a higher ionic conductivity than that of the PS additive copolymer electrolyte. From previous studies, a pure PS material exists a lower ionic conductivity about 10^{-12} S.cm^{-1}. However, it can enforce the strength of the PEO electrolyte. For the purpose of studying the influence of the PS addition to the PEO electrolyte, 0% to 70% of the PS weight percentages were simulated to predict the copolymer material performance. The resulting lithium ion diffusion coefficients and ionic conductivities under various PS wt% and different temperatures are shown in Figure 9 and Figure 10, respectively. The thermal effect is positive; however, both diffusion coefficients and ionic conductivities of the copolymer electrolyte decrease with increasing PS wt% proportion. The decreasing behavior of the ionic conductivity is attributed to the heavier molecular weight of the PS constituents; the carbon atoms and the heavy benzene ring will obstruct ionic transportation.

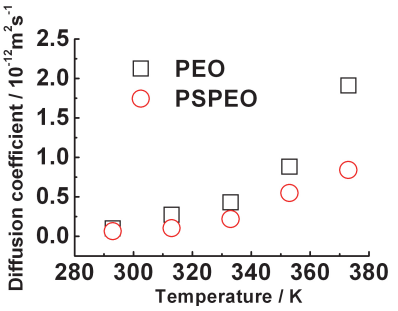

Figure 7: Diffusion coefficients of lithium ions in the PEO and in the PS-PEO versus operating temperature. The higher the temperature, the greater the diffusion coefficient.

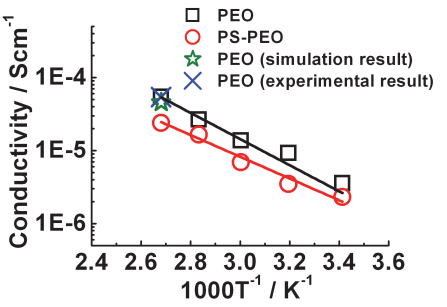

Figure 8: Arrhenius plot for the PEO and PS-PEO polymer electrolytes in this MD simulation. Another simulation result is obtained from Siqueira and Ribeiro (2006). The experimental result is extracted from Gorecki, Andreani, Berthier, Armand, Mali, Roos, and Brinkmann (1986). They show good agreement.

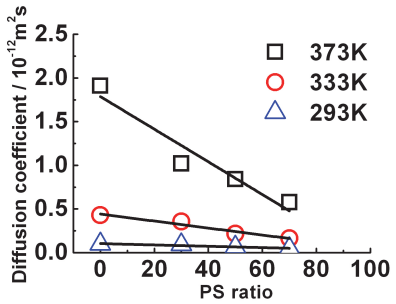

Figure 9: Diffusion coefficients of lithium ions at different PS ratios of the PS-PEO and at different operating temperatures. The thermal effect is positive; however, the diffusion coefficients of the copolymer electrolyte decrease with increasing PS wt% proportion.

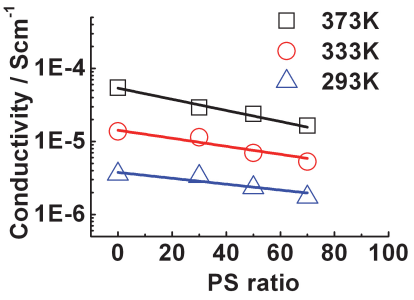

Figure 10: Ionic conductivities of lithium ions at different PS ratios of the PS-PEO and at different operating temperatures. The thermal effect is also positive; however, the ionic conductivities of the copolymer electrolyte decrease with increasing PS wt% proportion.

The molecular structure is able to be explained from the radial distribution function (RDF), which is defined as the local number density divided by the system density, and is employed to predict the conjugate probability between two species atoms. The probability of lithium ions to conjugate with carbon atoms in the PEO and in the PS-PEO is shown in Figure 11. The Li-C conjugation is observed to have a higher value in the PS-PEO than in the PEO. The first Li-C conjugation radius occurs in the PS-PEO at 2.5Å, whereas for PEO, it first occurs at a radius of 4.5Å. Indeed, the carbon atoms have a high attracting force that traps lithium ions, retarding ionic conduction. On the contrary, oxygen atoms play the role of delivering lithium ions, shown in Figure 12. The interactions between lithium ion and oxygen occur at a near distance and at a higher rate in the PEO than that in the PS-PEO, promoting ionic movements. The conjugate phenomenon between lithium ions and fluorides in the PS-PEO lowers the conduction rate of lithium ions in polymer electrolytes and is shown in Figure 13. Morphologies of different PS wt%, shown in Figure 14, reveal that obvious dispersion distributions take place in the PEO polymer electrolyte. On the contrary, the higher PS wt% displays a stronger gathering within the atomic forces. For this reason, lithium ions perform a better ability to transport through the PEO than in the PS-PEO.

Mechanical strength, for increasing durability, is an important issue of concern in the solid electrolyte membrane design. In this research, the mechanical properties of the electrolytes are evaluated through their dynamic behaviors. The execution procedure exerts stress forces in x, y, and z directions which are applied to the polymer materials. Convergence of distributions can be monitored and plotted in Figure 15. The required deformation potentials for constant motions are calculated and shown in Figure 16. It is noted that the PEO-based copolymer electrolyte with higher PS additive requires a higher potential force to cause deformation. The method to quantify the mechanical strength is through the evaluation of its Young's modulus, which is determined based on calculation of the total energy components that can be seen in Figure 17. The potential force resulted from the electrostatic interaction and the van der Waals (VDW) shows a significant influence on the polymer electrolytes than that of the kinetic energy. In the cases of PS wt% above 50%, shown in Figure 18, a dramatic increase in the force is observed in the PS-PEO copolymer electrolytes. The intra potential force resulted from charge interactions (apart from the VDW) constantly increases with higher PS wt%, evidently enhancing the mechanical strength of the PS-PEO copolymer electrolytes. Figure 19 reveals the bulk Young's modulus at different PS ratios which are estimated from the molecular simulations. Young's modulus of the PEO equals 0.05 GPa, which is comparable to the value of 0.0753 GPa obtained from experimental measurement by Yang, Shi, Pramoda, and Goh (2007). The slight disagreement between

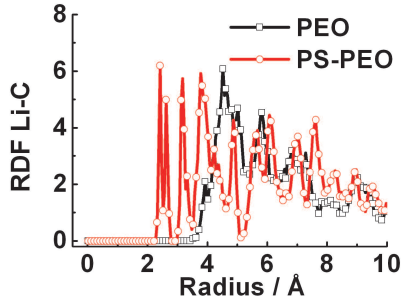

Figure 11: Radial distribution function (RDF) of Li-C distribution in the PEO and in the PS-PEO. The carbon atoms have a high attracting force that traps lithium ions, retarding ionic conduction.

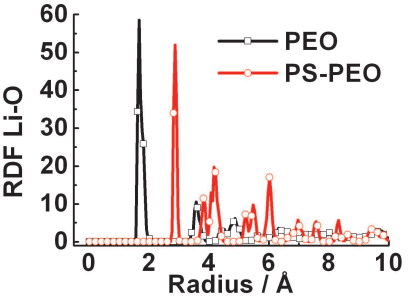

Figure 12: Radial distribution function (RDF) of Li-O distribution in the PEO and in the PS-PEO. The oxygen atoms play the role of delivering lithium ions.

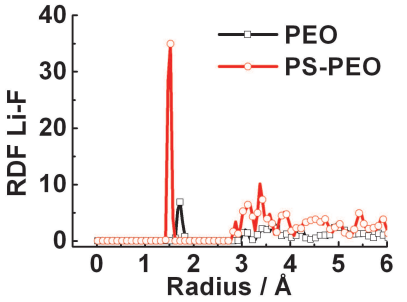

Figure 13: Radial distribution function (RDF) of Li-F distribution in the PEO and in the PS-PEO. The fluorides lower the conduction rate of lithium ions in polymer electrolytes.

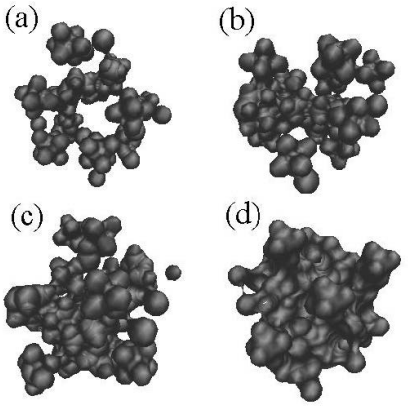

Figure 14: Morphologies of the PS-PEO of PS wt% (a) 0%, (b) 30%, (c) 50%, and (d) 70%. Obvious dispersion takes place in the PEO (0%-PS). Higher PS wt% displays a stronger gathering. Li ions perform a better ability to transport through the PEO than in the PS-PEO.

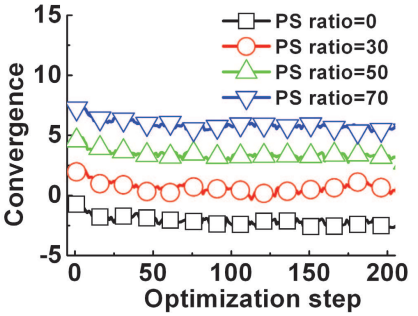

Figure 15: Stress-strain convergence (arbitrary units) at different PS in the optimization steps

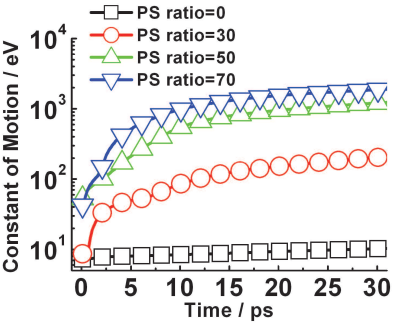

Figure 16: Deformation potentials (eV) for constant motions at different PS ratios within the observation period. The PEO-based copolymer electrolyte with higher PS additive requires a higher potential force to cause deformation.

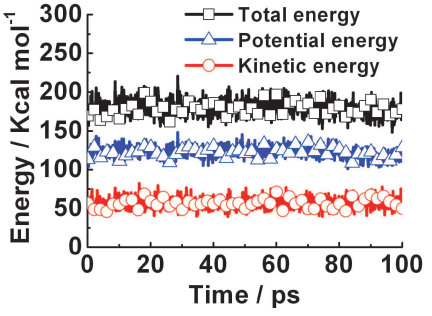

Figure 17: Kinetic energy, potential energy, and total energy distributions in the simulation period. The potential force resulted from the molecular interaction shows a significant influence on the polymer electrolytes than that of the kinetic energy.

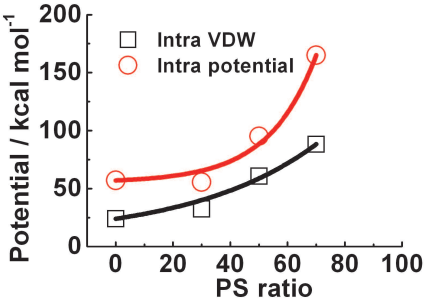

Figure 18: Intra van der Waals force and intra potential at different PS ratios. The intra potential force resulted from charge interactions (apart from the VDW) constantly increases with higher PS wt%, hence, enhances the mechanical strength of the PS-PEO copolymer.

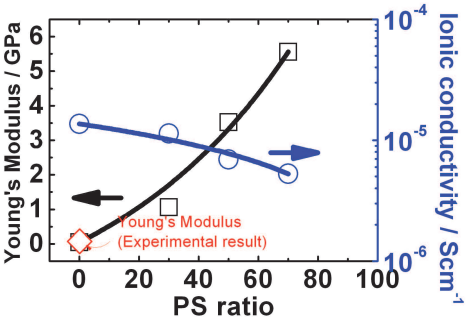

Figure 19: Young's modulus and ionic conductivity at different PS ratios. The experimental result is extracted from Yang, Shi, Pramoda, and Goh (2007). The trend of the Young's modulus displays the strengthened PS-PEO attained by adding a larger proportion of PS mixtures at the cost of decreasing ionic conductivity. The compromise between an acceptable ionic conductivity and a required mechanical strength shows at the PS ratio around 40% to 50%.

experimental and simulation values is due to the finite number of polymer constituents employed in the simulation. The trend of the Young's modulus displays the strengthened PS-PEO attained by adding a larger proportion of PS mixtures. In addition, PS additives diminish the ionic conductivity of the copolymer electrolyte. The compromise between an acceptable ionic conductivity and a required mechanical strength shows at the PS ratio around 40% to 50%.

4 Conclusions

This paper has employed molecular dynamics (MD) simulation techniques to predict the ionic characteristics and molecular strengths in the poly(ethylene oxide) (PEO) and in the poly(styrene-b-ethylene oxide) (PS-PEO) molecular systems. The results reveal that ionic transport is easier in PEO than in PS-PEO at different temperatures. In addition, MD simulation was also employed to determine the mechanical strength of the PEO based polymer electrolytes with different PS wt% in PS/PEO mixtures. Young's modulus of the copolymer electrolytes shows a dramatic increase at higher PS wt%. This behavior was explained from an analysis of intra van der Waals (VDW) force and intra potential force based on atomic interactions. The results indicated that PS can efficiently enhance the mechanical properties of the PEO polymer electrolytes in stress and strain behaviors, but at the expense of a lower ionic conductivity. The compromise shows at the PS ratio around 40-50%. It has been developed an equilibrium PS/PEO mixture to meet

an acceptable ionic conductivity and a required mechanical strength. This study provides the first indication to achieve conductive and mechanical requirements at different operating conditions using computer simulations, instead of try-and-error experiments.

Acknowledgement: Thanks are due to the National Science Council of Taiwan and the Energy Bureau of DOE who supported this research under the grant number: NSC 100-2623-E-007-009-ET. We are also grateful to the National Center for High-Performance Computing (NCHC) for the generous computer time and facilities.

References

Allen, M.P.; Tildesley, D.J. (1987): *Computer simulation of liquids*, Oxford University Press, New York.

Andreev, Y.G.; Bruce, P.G. (2000): Polymer electrolyte structure and its implications, *Electrochimica Acta*, vol. 45, pp. 1417-1423.

Berendsen, H.J.C.; Grigera, J.R.; Straatama, T.P. (1987): The missing term in effective pair potentials, *J. Phys. Chem.*, vol. 91, pp. 6269-6271.

Borodin, O.; Douglas, R.; Smith, G.D.; Trouw, F.; Petrucci, S. (2003): MD simulations and experimental study of structure, dynamics, and thermodynamics of poly(ethylene oxide) and its oligomers, *J. Phys. Chem. B*, vol. 107, pp. 6813-6823.

Boschet, F.; Branger, C.; Margaillan, A. (2003): Synthesis and characterization of PS-block-PEO associative water-soluble polymers, *European Polymer Journal*, vol. 39, pp. 333–339.

Brandell, D.; Liivat, A.; Kasema, H.; Aabloo, A.; Thomas, J.O. (2005): Molecular dynamics simulation of the $LiPF_6{\cdot}PEO_6$ structure, *J. Mater. Chem.*, vol. 15, pp. 1422-1428.

Brodeck, M.; Alvarez, F.; Arbe, A.; Juranyi, F.; Unruh, T.; Holderer, O.; Colmenero, J.; Richter, D. (2009): Study of the dynamics of poly(ethylene oxide) by combining molecular dynamic simulations and neutron scattering experiments, *J. Chem. Phys.*, vol. 130, 094908(1-14).

Chen, W.H.; Hong, C.W. (2011): Nano-array solid electrode design for photoelectrochemical solar cells, *CMC: Computer, Materials, & Continua,* vol. 20, pp. 1-24.

Diddens, D.; Heuer, A.; Borodin, O. (2010): Understanding the lithium transport within a rouse-based model for a PEO/LiTFSI polymer electrolyte, *Macro-*

molecules, vol. 43, pp. 2028-2036.

Ennari, J.; Neelov, I.; Sundholm, F. (2000): Molecular dynamics simulation of the structure of PEO based solid polymer electrolytes, *Polymer*, vol. 41, pp. 4057-4063.

Ennari, J.; Pietila, L.O.; Virkkunen, V.; Sundholm, F. (2002): Molecular dynamics simulation of the structure of an ion-conducting PEO-based solid polymer electrolyte, *Polymer*, vol. 43, pp. 5427–5438.

Fullerton-Shirey, S.K.; Maranas, J.K. (2009): Effect of $LiClO_4$ on the structure and mobility of PEO-based solid polymer electrolytes, *Macromolecules*, vol. 42, pp. 2142-2156.

Gadjourova, Z.; Andreev, Y.G.; Tunstall, D.P.; Bruce, P.G. (2001): Ionic conductivity in crystalline polymer electrolytes, *Nature*, vol. 412, pp. 520-523.

Gorecki, W.; Andreani, R.; Berthier, C.; Armand, M.; Mali, M.; Roos, J.; Brinkmann, D. (1986): NMR, DSC, and conductivity study of a poly (ethylene oxide) complex electrolyte: $PEO(LiClO_4)_x$, *Solid State Ionics*, vol. 295, pp. 18-19.

Grujicic, M.; Chittajallua, K.M.; Cao, G.; Roy, W.N. (2005): An atomic level analysis of conductivity and strength in poly(ethylene oxide) sulfonic acid-based solid polymer electrolytes, *Materials Science and Engineering B*, vol. 117, pp. 187-197.

Hektor, A.; Klintenberg, M.K.; Aabloo, A.; Thomas, J.O. (2003): Molecular dynamics simulation of the effect of a side chain on the dynamics of the amorphous $LiPF_6$–PEO system, *J. Mater. Chem.*, vol. 13, pp. 214-218.

Hong, C-W; Tsai, C-Y(2010): Computational Quantum Mechanics Simulation on the Photonic Properties of Group-III Nitride Clusters, *CMES: Computer Modeling in Engineering & Sciences*, Vol. 67, No. 2, pp. 79-94.

Hypercube Inc., (2002): HyperChem reference manual. Chapter 8.

Karan, N.K.; Pradhan, D.K.; Thomas, R.; Natesan, B.; Katiyar, R.S. (2008): Solid polymer electrolytes based on polyethylene oxide and lithium trifluoro-methane sulfonate (PEO-$LiCF_3SO_3$) Ionic conductivity and dielectric relaxation, *Solid State Ionics*, vol. 179, pp. 689– 696.

Lee, S.F.; Hong, C.W. (2009): Computer modeling of ionic conductivity in low temperature doped ceria solid electrolytes, *CMC: Computer, Materials, & Continua,* vol. 12, pp. 223–235.

Li, D.; Saheli, G.; Khaleel, M.; Garmestani, H. (2006): Microstructure optimization in the fuel cell electrodes using materials design, *CMC: Computer, Materials, & Continua,* vol. 4, pp. 31–42.

Liivat, A.; Brandell, D.; Thomas, J.O. (2007): A molecular dynamics study of

ion-conduction mechanisms in crystalline low-Mw $LiPF_6 \cdot PEO_6$, *J. Mater. Chem.*, vol. 17, pp. 3938–3946.

Mayo, S.L.; Olfason, B.D.; Goddard, W.A. (1990): Dreiding - a generic force-field for molecular simulations, *J. Phys. Chem.*, vol. 94, pp. 8897-8909.

Neto, C.; James, M.; Telford, A.M. (2009): On the composition of the top layer of microphase separated thin PS-PEO films, *Macromolecules*, vol. 42, pp. 4801–4808

Ogawa, T.; Miyano, M.; Suzuki, Y.; Suzuki, A.; Tsuboi, H.; Hatakeyama, N. Endou, A.; Takaba, H.; Kubo, M.; Miyamoto, A. (2010): A theoretical study on initial processes of Li-ion transport at the electrolyte/cathode interface a quantum chemical molecular dynamics approach, *Japanese Journal of Applied Physics,* vol., 49, 04DP11 (1-6).

Rejsek, V.; Desbois, P.; Deffieux, A.; Carlotti, S. (2010): Polymerization of ethylene oxide initiated by lithium derivatives via the monomer-activated approach: Application to the direct synthesis of PS-b-PEO and PI-b-PEO diblock copolymers, *Polymer*, vol. 51, pp. 5674-5679.

Ryckaert, J.P.; Ciccotti, G.; Berendsen, H.J.C. (1977): Numerical-integration of cartesian equations of moion of a system with constraints-molecular-dynamics of N-alkanes, *J. Comput. Phys.*, vol. 23, pp. 327-341.

Shen, S.; Atluri, S.N. (2004): Atomic-level stress calculation and continuum-molecular system equivalence, *CMES: Computer Modeling in Engineering & Sciences,* vol. 6, pp. 91-104.

Siqueira, L.J.A.; Ribeiro, M.C.C. (2005): Molecular dynamics simulation of the polymer electrolyte PEO/$LiClO_4$. I. Structural properties, *J. Chem. Phys.*, vol. 122, pp. 194911 (1-8).

Siqueira, L.J.A.; Ribeiro, M.C.C. (2006): Molecular dynamics simulation of the polymer electrolyte PEO/$LiClO_4$. II. Dynamical properties, *J. Chem. Phys.*, vol. 125, pp. 214903 (1-8).

Smith, W.; Leslie, M.; Forester, T.R. (2003): The DL_POLY user manual, CCLRC, Daresbury Laboratory.

Suga, K; Ito, T(2010): Lattice Boltzmann Flow Models for Micro/Nano Fluidics, *CMES: Computer Modeling in Engineering & Sciences*, Vol. 63, No. 3, pp. 223-242.

Verlet, L. (1967): Computer experiments on classical fluids .I. thermodynamical properties of Lennard-Jones moleculars, *Phys. Rev.*, vol. 159, pp. 98-103.

Yang, B.X.; Shi, J.H.; Pramoda, K.P.; Goh, S.H. (2007): Enhancement of stiffness, strength, ductility and toughness of poly(ethylene oxide) using phenoxy-grafted multiwalled carbon nanotube, *Nanotechnologys*, vol. 18, pp. 125606-

125612.

Yang, P.; Han, Y. (2009): Microphase-separated brushes on square platelets in PS-b-PEO thin films, *Macromolecules Rapid Communion*, vol. 30, pp. 1509–1514

Yang, P.; Yu, X.; Han, Y. (2010): Transition between crystallization and microphase separation in PS-b-PEO thin film influenced by solvent vapor selectivity, *Polymer*, vol. 51, pp. 4948-4957

Young, W.S.; Epps, T.H. (2009): Salt doping in PEO-containing block copolymers counterion and concentration effects, *Macromolecules*, vol. 42, pp. 2672-2678.